FUSE Spectra of the Black Hole Binary LMC X-3[1]

J.B. Hutchings, K. Winter

Herzberg Institute of Astrophysics, National Research Council of Canada,

5071 W. Saanich Rd., Victoria, B.C. V9E 2E7, Canada

email john.hutchings@nrc-cnrc.gc.ca

A.P. Cowley, P.C. Schmidtke

Department of Physics & Astronomy, Arizona State University, Tempe, AZ, 85287-1504

and

D. Crampton

Herzberg Institute of Astrophysics, National Research Council of Canada,

5071 W. Saanich Rd., Victoria, B.C. V9E 2E7, Canada

Received _____; accepted _____

[1]Based on observations made with the NASA-CNES-CSA Far Ultraviolet Spectroscopic Explorer. FUSE is operated for NASA by Johns Hopkins University under NASA contract NAS 5-3298

ABSTRACT

Far-ultraviolet spectra of LMC X-3 were taken covering photometric phases 0.47 to 0.74 in the 1.7-day orbital period of the black-hole binary (phase zero being superior conjunction of the X-ray source). The continuum is faint and flat, but appears to vary significantly during the observations. Concurrent *RXTE*/ASM observations show the system was in its most luminous X-ray state during the FUSE observations. The FUV spectrum contains strong terrestrial airglow emission lines, while the only stellar lines clearly present are emissions from the O VI resonance doublet. Their flux does not change significantly during the FUSE observations. These lines are modelled as two asymmetrical profiles, including the local ISM absorptions due to C II and possibly O VI. Velocity variations of O VI emission are consistent with the orbital velocity of the black hole and provide a new constraint on its mass.

Subject headings: X-rays: binaries – stars: individual: (LMC X-3)

1. Introduction

LMC X-3 is one of the brightest X-ray sources in the Large Magellanic Cloud, with $L_X > 10^{38}$ erg s^{-1}. It shows both high/soft and low/hard X-ray states. Spectroscopic observations of the B3 V star revealed an orbital period of ~ 1.7 days and an unseen massive companion which was interpreted as a $\sim 10 M_\odot$ black hole (Cowley et al. 1983). Subsequent optical photometry (van der Klis et al. 1985; Kuiper et al. 1988) showed ellipsoidal variations ($\Delta m \sim 0.2$ mag) of the B star, which improved the ephemeris and also indicated a large mass for the secondary star. Ultraviolet spectra taken with HST showed a moderate strength N V, 1240Å, emission line and weak emissions of C IV, 1550Å, and He II, 1640Å (Cowley et al. 1994). These lines appeared to be formed in the accretion disk surrounding the black hole, but only two spectra were obtained and it was not possible to determine their velocity amplitude. Given the strength of N V, we expected the resonance lines of O VI to be detectable with FUSE spectra. The properties of these lines might provide further information about the accretion disk and motion of the black hole.

2. FUSE Observations

LMC X-3 was observed through 8 consecutive FUSE orbits, yielding spectra centered at binary phases 0.47 through 0.74, thus covering about a quarter of the orbit beginning slightly before the inferior conjunction of the X-ray source. The observations were taken through the large science aperture and are summarized in Table 1. Spectra were extracted using the standard FUSE pipeline procedure.

The continuum is weak across the FUSE bandpass, with flux roughly flat at 8×10^{-15} erg s^{-1} cm^{-2} $Å^{-1}$. One FUSE channel (SiC A) shows no continuum, which probably means the alignment was not good for that telescope. All channels show a rich emission-line

spectrum of H I and O I, which arises from terrestrial airglow. The zero radial velocity of these emission lines confirms this origin. The strength of these lines changes from day to night (O I drops more than H I at night), so in Table 1 we have indicated what percentage of each observation was taken during nighttime. The observations were taken with a single pointing with re-acquisitions after earth-occultations, so the different FUSE channels should have had stable alignment throughout the observations.

The presence of the airglow lines makes it difficult to detect many of the principal high ionization lines that may be present in the LMC X-3 spectrum, such as C III, 977Å, N III, 992Å, and He II, 1085Å. However, if present, they are very weak. There is a possible weak broad feature at C III, 1175Å, and a possible feature at ∼1000Å which is clear of airglow but has no obvious identification. However, the principal feature of the spectrum is the O VI doublet, which is stronger than any of the other lines and mostly not overlaid by airglow emission. The far ultraviolet spectrum of LMC X-3 is shown in Figure 1.

3. Concurrent X-ray Data

We have also extracted the *RXTE* All Sky Monitor (ASM) data from the publicly available web site. These data are shown in Figure 2, with the time of the FUSE observations indicated. LMC X-3 is known to vary considerably in its X-ray flux, and the figure shows that the FUSE data were obtained when the source was in its brightest X-ray phase. We note that early observations suggested the occurence of the high/low states might be periodic (Cowley et al. 1991), but this has been demonstrated not to be the case (e.g. Wilms et al. 2001; Brocksopp, Groot, & Wilms 2001). These authors find that the optical and X-ray light curves are correlated, with the X-rays slightly lagging in time, implying a variable mass-accretion rate model rather than disk precession.

4. FUSE Measurements

Table 1 gives the measures of the continuum and O VI line flux from the FUSE spactra. The continuum was estimated from the LiF channels 1a, 2a, and 2b (1b has the 'worm' grid wire shadow that masks some flux), after removing the airglow emission lines. The variations are seen in all three channels and so are considered real. The absolute level of the continuum is less certain because of the difficulty in extracting background and detector systematics at this low flux level. The general nature of the changes are a ∼20% rise in spectrum through phase 0.64, followed by a steady drop by a factor ∼ 2 over the last three spectra. These relative changes in the continuum have scatter of less than 20% after the mean levels have been normalized.

The O VI line flux was measured from all four FUSE channels that cover this wavelength range, with greater weight on the LiF channels. There is considerable noise and strong C II absorption within the profile, so the numbers given have standard deviations of about 15%. Thus, there is no significant variation in the O VI flux, although there is a suggestion that the line strength rises and then falls in phase with the continuum.

5. Discussion

The continuum changes occur over binary phases where the accreting black hole moves from inferior conjunction to quadrature. At these phases, a disk thickening at the impact point of the mass-transfer stream would move from illuminated to partially covering the disk, which could account for the observed drop in far-UV flux. However, there may also be non-phased changes on this timescale. The only way to clarify the matter would be to obtain observations that cover additional binary phases, as well as several orbital cycles. The small O VI flux changes may occur in the unocculted central parts of the accretion

disk.

The optical ellipsoidal light curve has an amplitude of ∼0.2 mag (van der Klis et al. 1985), while a small amount of data in the UV from HST shows a similar range. The orbital X-ray flux changes are smaller (Boyd, Smale, & Dolan 2001). Thus, the indicated large flux range reported here in the FUV has not been seen at other wavelengths.

If O VI emission arises in the inner disk, it should show the orbital motion of the black hole. Before looking for line shifts, we need to understand the observations in more detail. Figures 3 and 4 display the O VI region in different ways and show that there are strong absorptions at 1036-7Å from C II. These are close to their rest wavelengths, so they are identified as Galactic ISM features. Figure 4 also shows O VI absorptions at their rest wavelengths (one is blended with C II, but the relative line strengths are consistent with that). Thus, in looking for line shifts from LMC X-3, we need to ignore these local absorption components. (It is of interest to note the apparent narrow O VI absorber at rest velocity. It is unlikely to arise near LMC X-3 in an outflow at exactly the velocity of LMC X-3 with respect to us, so it must arise in the hot ISM of the Galaxy.)

In Figure 4, we show a possible way to model the O VI line emission. We have used just the LiF1a channel data for this, as it has the highest S/N and has the most reliable wavelength scale, being the guide channel. The emission is assumed to have an aymmetrical profile defined by the long wavelength tail and the shortward cutoff of the whole feature. We further assume the two O VI lines have identical profiles, that their strengths have roughly the ratio of 2 expected for optically thin emission, and that the peaks are centered at the systemic velocity of LMC X-3 (+310 km s^{-1}). The result, shown in Figure 4, fits the overall profile well. It is possible to fit the data with symmetrical profiles too, but this would require a different identification for the emission longward of 1042Å, and none is obvious.

To look for velocity changes, we summed spectra into two phase bins, as illustrated in Figure 3, since the spectra are too noisy to measure individually. The bins are centered at phases 0.53 and 0.70. Velocity shifts between the two phase bins were measured by: a) fitting of profiles as shown in Figure 4; b) cross-correlation between them and the overall mean, both with the C II absorptions in and edited out; and c) hand overlay of the plotted profiles, filtering the absorbers out visually. We also worked with both the LiF1a alone, and sum of all channel spectra. In all measurements, we found the 0.53-phase bin to have a more negative velocity than the 0.70-phase bin, with the velocity difference being in the range 100-150 km s^{-1}. When we fit a sine curve to this difference, imposing the phasing for expected orbital motion of the black hole, we find an orbital semiamplitude, K_{bh}, in the range of 130-200 km s^{-1}. Cowley et al. (1983) found K_B=235 km s^{-1} from measuring the B star's velocities. Hence, the FUSE results suggest the black hole may be more massive than the optically visible star. The implied mass ratio lies in the range $0.55-0.83$. Adopting the highest of these values, we derive minimum masses of 15 and 13 $M_\odot$ for the black hole and B star, respectively.

We note that Soria et al. (2001) suggest that the velocity amplitude derived by Cowley et al. may be overestimated by $\sim 15\%$ due to possible line weakening on the X-ray heated face of the B star. However, this scenario would require a significant modulation of the spectrum with phase, which is not observed. A plot of the equivalent widths of both the hydrogen and He I lines versus phase (using those tabulated by Cowley et al., and orbital phases computed using the ephemeris of van der Klis et al.) shows that there is no orbital trend in the strength of these lines. As noted by Cowley et al., all lines are weakened compared to a normal B star, presumably because of the additional continuum from the accretion disk. However, the ratio of H to He I line strengths is similar to that in normal single B stars. On the other hand, it is possible that the B-star velocity semiamplitude might instead be underestimated if the heating effect causes one to observe more spectral

light from the B star's inner hemisphere.

Our FUSE measurement from averaged spectra of only two emission velocites, which are thought to arise in the black hole's accretion disk, is far from a conclusive determination of the mass ratio in LMC X-3. However, it does suggest that full orbital observations of UV emission lines could help to define the range of possible masses in this system. Thus, while the FUSE data are quite limited, they are consistent with the O VI emission originating in the inner parts of the accretion disk and provide a direct estimate of the mass ratio for the first time. Further orbital coverage by FUSE would provide much more definitive mass estimates.

The authors acknowledge the use of the *RXTE*-ASM data from the web site. In addition, APC thanks NASA for partial support of this research.

Table 1. FUSE Observations of LMC X-3

MJD (mid-exp)	Exp time (sec)	% Obs at night	Φ_{phot}[a]	Continuum (erg s^{-1} cm^{-2} Å^{-1})	O VI emission (erg s^{-1} cm^{-2})
52228.742	2929	69	0.47	6.7×10^{-15}	8.1×10^{-14}
52228.813	2673	64	0.52	7.1×10^{-15}	7.1×10^{-14}
52228.884	2467	60	0.56	7.6×10^{-15}	9.5×10^{-14}
52228.956	2262	53	0.60	7.2×10^{-15}	8.8×10^{-14}
52229.027	2153	46	0.64	9.1×10^{-15}	8.8×10^{-14}
52229.108	4059	24	0.69	7.0×10^{-15}	9.1×10^{-14}
52229.154	3942	54	0.72	5.5×10^{-15}	8.1×10^{-14}
52229.200	3942	28	0.74	3.9×10^{-15}	7.5×10^{-14}

[a] Photometric ephemeris: HJD 2445278.005 + 1.70479E (MJD 45277.505), where Φ=0 is superior conjunction of black hole (from van der Klis et al. 1985)

REFERENCES

Boyd, P.T., Smale, A.P., & Dolan, J.F. 2001, ApJ, 555, 822

Brocksopp, C., Groot, P.J., & Wilms, J. 2001, MNRAS, 328, 139

Cowley, A.P., Crampton, D., Hutchings, J.B., Remillard, R., & Penfold, J.E. 1983, ApJ, 272, 118

Cowley, A.P., Schmidtke, P.C., Ebisawa, K., Makino, F., Remillard, R.A., Crampton, D., Hutchings, J.B., Kitamoto, S., & Treves, A. 1991, ApJ, 381, 526

Cowley, A.P., Schmidtke, P.C., Hutchings, J.B., & Crampton, D. 1994, ApJ, 429, 826

Kuiper, L., van Paradijs, J., & van der Klis, M. 1988, A&A, 203, 79

Soria, R., Wu, K., Page, M.J., & Sakelliou, I. 2001, A&A, 365, L273

van der Klis, M., Clausen, J.V., Jensen, K., Tjemkes, S., & van Paradijs, J. 1985, A&A, 151, 322

Wilms, J., Nowak, M.A., Pottschmidt, K., Heindl, W.A., Dove, J.B., & Begelman, M.C. 2001, MNRAS, 320, 327

Fig. 1.— Overall spectrum of LMC X-3, from the best FUSE channels. The shorter wavelengths (top panel) have more smoothing for easier visibility. The sharp emission lines are all airglow, and they are broadened by the smoothing. The positions of the high ionization emission lines seen in accretion disk systems are marked (at LMC shifted wavelengths). Only O VI is definitely present. Both LiF channels are plotted in this region to show the detailed agreement.

Fig. 2.— *RXTE* All Sky Monitor X-ray data for LMC X-3 covering ∼8 years of observations. The date of the FUSE observations presented in this paper is marked.

Fig. 3.— O VI emission region, overall and in two binary phase bins. The lower panel shows the difference between the two phase-binned spectra. The dotted lines indicate the regions where airglow emission has been edited out. These spectra are derived from all FUSE channels.

Fig. 4.— Mean O VI LiF1a profile with fitted profiles of the doublet (shown by the lighter weight lines - see text). Dashed line shows the residual spectrum after subtraction of model profiles. The positions of local absorbers of C II and O VI are marked.

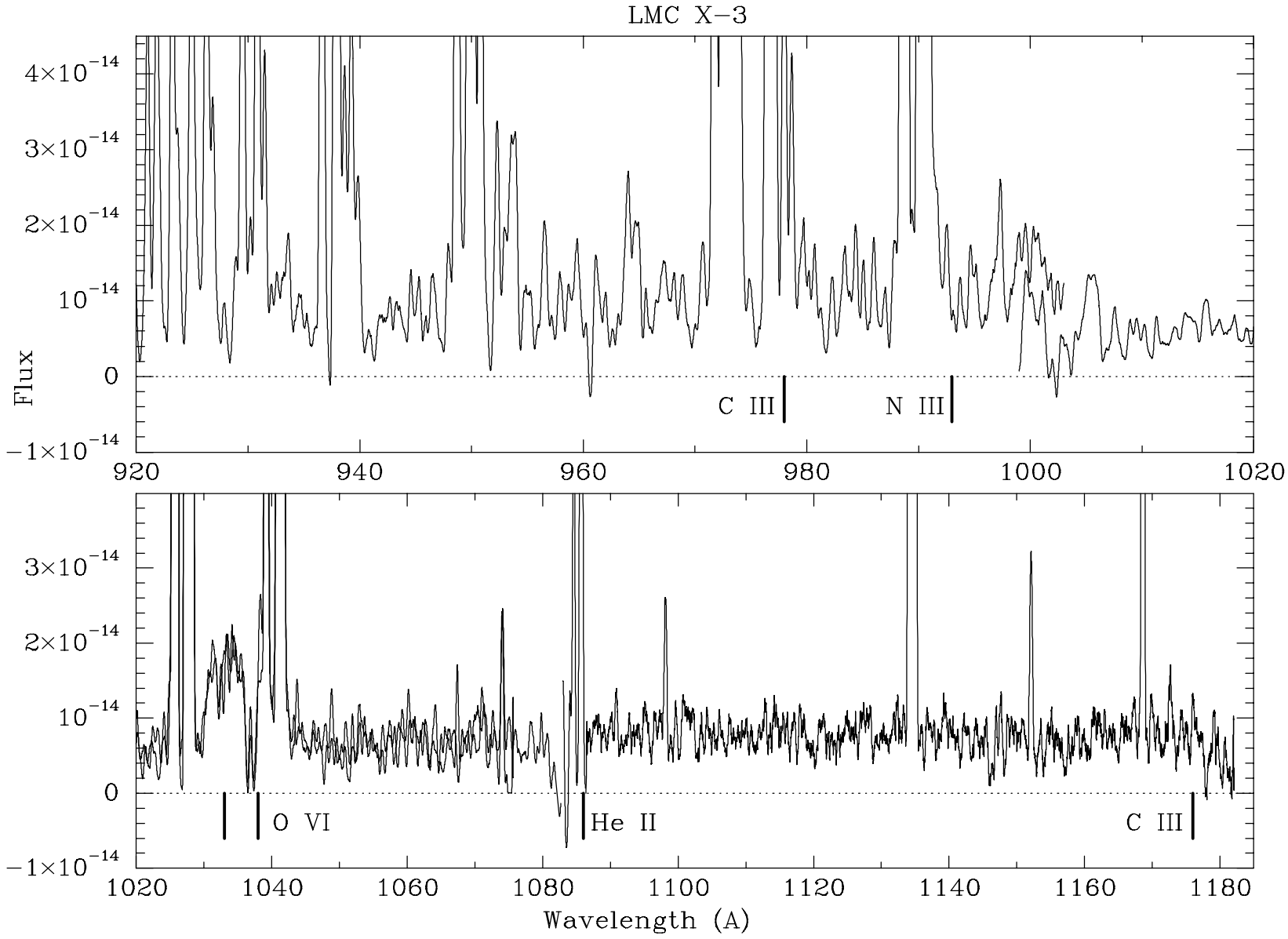
LMC X−3
Flux
4×10^−14
3×10^−14
2×10^−14
10^−14
0
−1×10^−14
C III
N III
O VI
He II
C III
920
940
960
980
1000
1020
1040
1060
1080
1100
1120
1140
1160
1180
Wavelength (A)

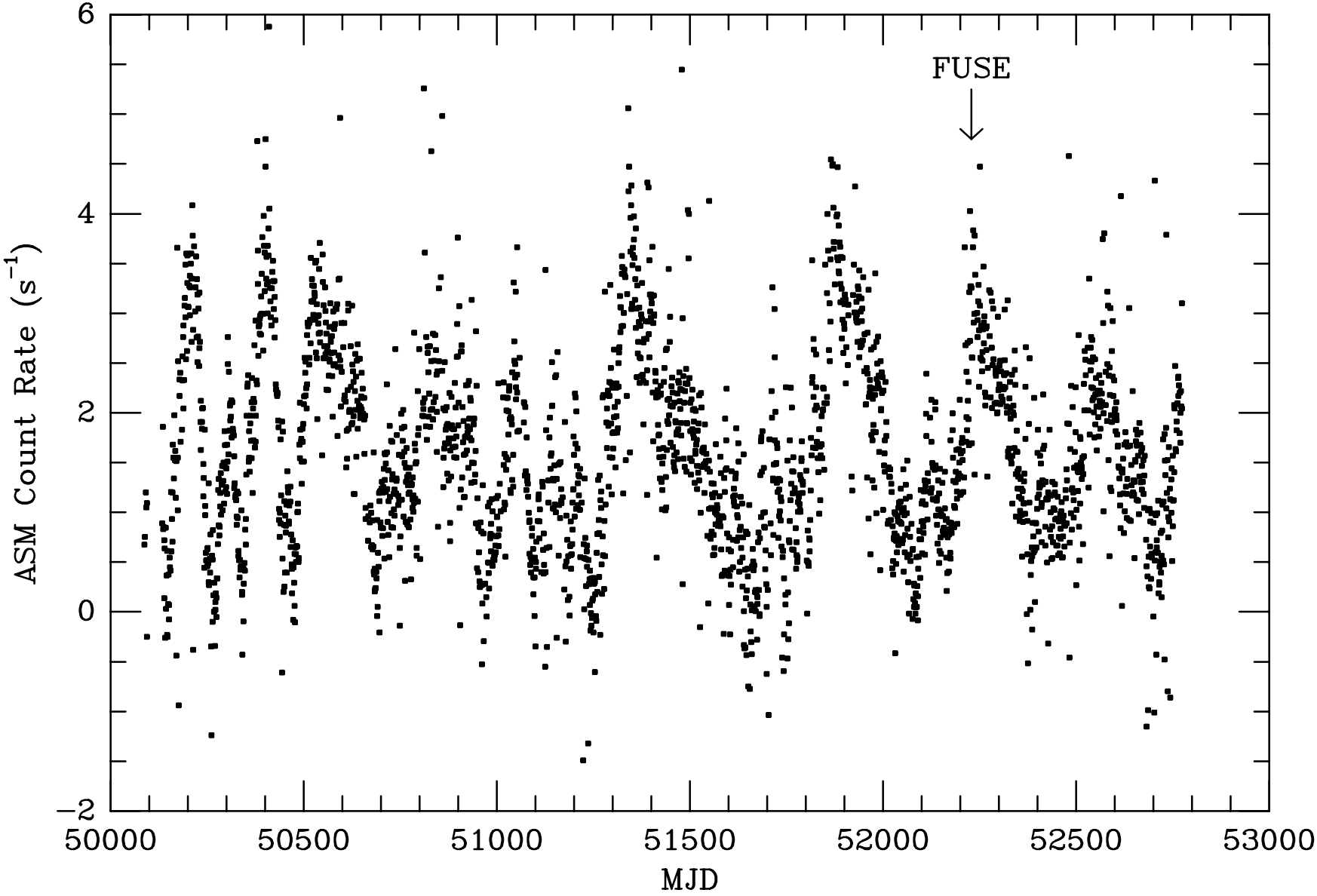
FUSE
ASM Count Rate (s^{-1})
MJD
6
4
2
0
−2
50000
50500
51000
51500
52000
52500
53000

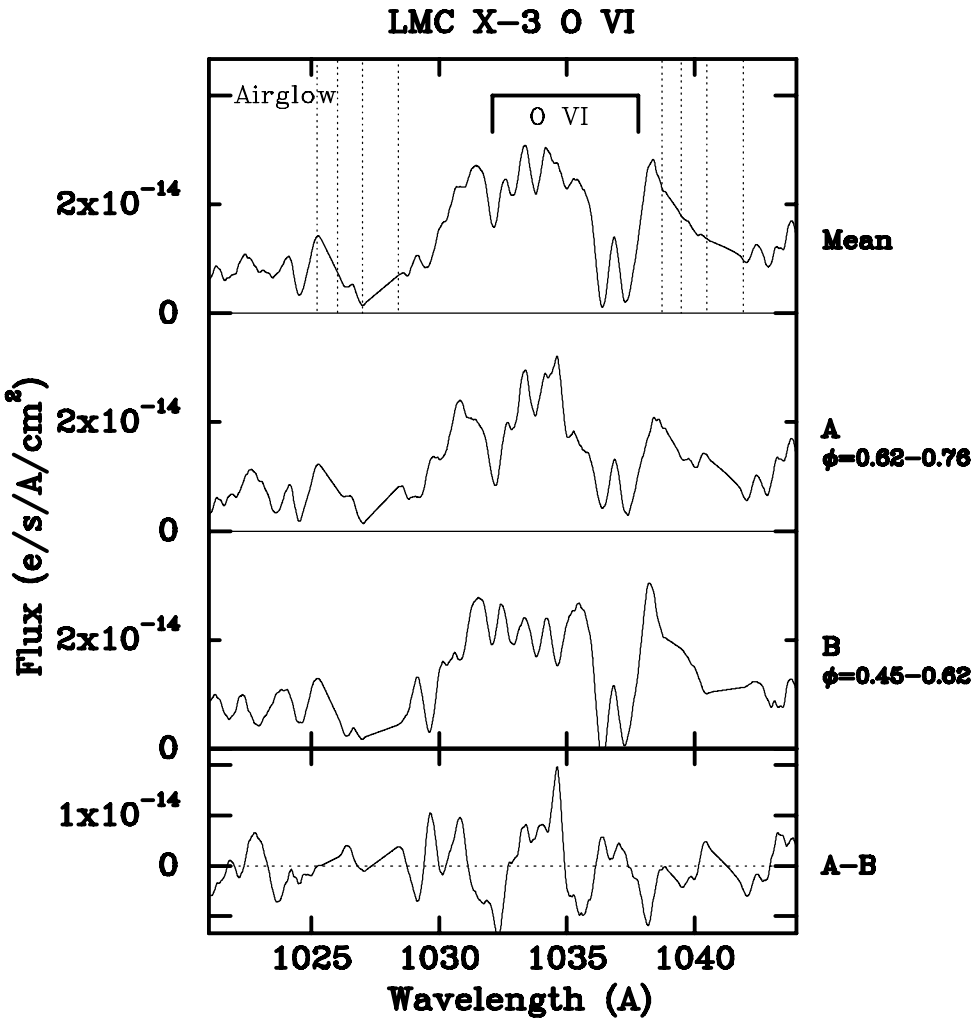
LMC X-3 O VI
Airglow
O VI
2x10^-14
0
Mean
2x10^-14
0
A
φ=0.62-0.76
2x10^-14
0
B
φ=0.45-0.62
1x10^-14
0
A-B
Flux (e/s/A/cm^2)
1025
1030
1035
1040
Wavelength (A)

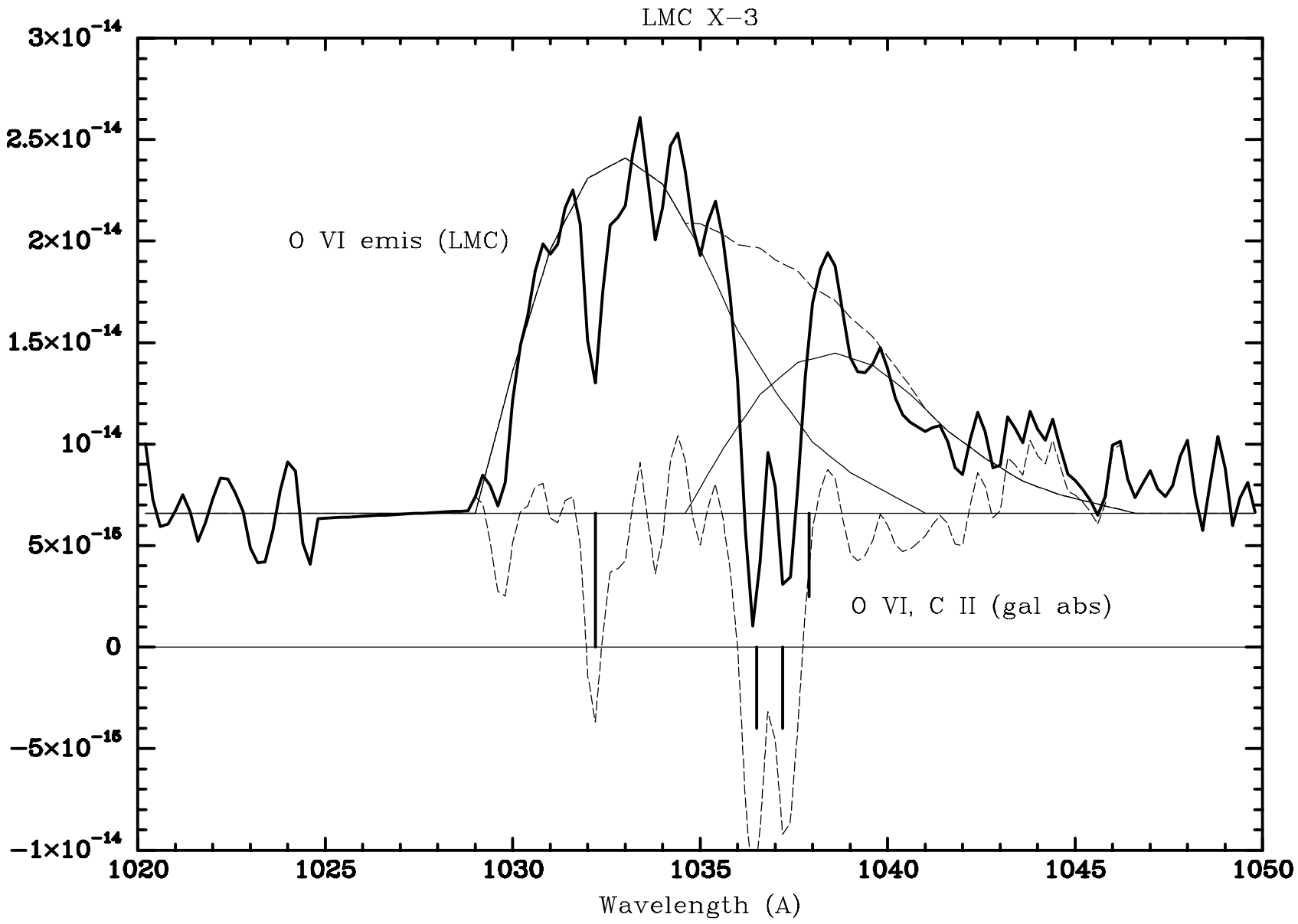
LMC X-3
O VI emis (LMC)
O VI, C II (gal abs)
3×10^-14
2.5×10^-14
2×10^-14
1.5×10^-14
10^-14
5×10^-15
0
-5×10^-15
-1×10^-14
1020
1025
1030
1035
1040
1045
1050
Wavelength (A)